The control of axillary meristem fate in the maize *ramosa* pathway

Andrea Gallavotti[1,*], Jeff A. Long[2], Sharon Stanfield[1], Xiang Yang[3], David Jackson[4], Erik Vollbrecht[3] and Robert J. Schmidt[1,*]

SUMMARY

Plant axillary meristems are composed of highly organized, self-renewing stem cells that produce indeterminate branches or terminate in differentiated structures, such as the flowers. These opposite fates, dictated by both genetic and environmental factors, determine interspecific differences in the architecture of plants. The Cys_2-His_2 zinc-finger transcription factor RAMOSA1 (RA1) regulates the fate of most axillary meristems during the early development of maize inflorescences, the tassel and the ear, and has been implicated in the evolution of grass architecture. Mutations in *RA1* or any other known members of the *ramosa* pathway, *RAMOSA2* and *RAMOSA3*, generate highly branched inflorescences. Here, we report a genetic screen for the enhancement of maize inflorescence branching and the discovery of a new regulator of meristem fate: the *RAMOSA1 ENHANCER LOCUS2* (*REL2*) gene. *rel2* mutants dramatically increase the formation of long branches in ears of both *ra1* and *ra2* mutants. *REL2* encodes a transcriptional co-repressor similar to the TOPLESS protein of *Arabidopsis*, which is known to maintain apical-basal polarity during embryogenesis. *REL2* is capable of rescuing the embryonic defects of the *Arabidopsis topless-1* mutant, suggesting that *REL2* also functions as a transcriptional co-repressor throughout development. We show by genetic and molecular analyses that REL2 physically interacts with RA1, indicating that the REL2/RA1 transcriptional repressor complex antagonizes the formation of indeterminate branches during maize inflorescence development. Our results reveal a novel mechanism for the control of meristem fate and the architecture of plants.

KEY WORDS: Maize *ramosa* pathway, Transcriptional repression, Axillary meristems

INTRODUCTION

Meristems are the reservoirs of stem cells that are responsible for the post-embryonic development of plants (Sablowski, 2007a). After germination, plants continuously form, in the axils of true or modified leaves, axillary meristems that can remain quiescent, or create either branches or flowers. The number, position and fate of these meristems are responsible for the variability observed in the architectures of different plant species (McSteen and Leyser, 2005; Sablowski, 2007b). Plant architecture, which is often modified during the domestication of crop species, is still a major target of selection in current breeding programs, as it influences the productivity and the mechanization requirements of modern farming. In maize, a major crop species, two types of axillary meristems are evident in the very early development of its reproductive structures, the tassel and the ear (Fig. 1A,C). In the tassel, the apical male inflorescence, the first axillary meristems formed are indeterminate, produce long branches and are therefore called branch meristems (Fig. 1E). The majority of axillary meristems, which are formed shortly afterwards, are instead determinate meristems that eventually terminate with the formation of a pair of spikelets (grass-specific structures containing flowers), and are therefore called spikelet-pair meristems (Fig. 1E). In the female inflorescence, the ear, only spikelet-pair meristems form in the early stages of development (Fig. 1G) (McSteen et al., 2000).

In the *ramosa1* (*ra1*), *ramosa2* (*ra2*) and *ramosa3* (*ra3*) mutants of maize, spikelet-pair meristems assume the identity and fate of branch meristems (Vollbrecht et al., 2005; Bortiri et al., 2006; Satoh-Nagasawa et al., 2006), and give rise to highly branched inflorescences. Both *RA1* and *RA2* encode plant-specific putative transcription factors, a Cys2-His2 zinc-finger protein of the EPF class and a LOB-domain-containing transcription factor, respectively (Vollbrecht et al., 2005; Bortiri et al., 2006). *RA3* instead encodes a metabolic enzyme, a trehalose-6-phosphate-phosphatase, and it is proposed to function through the modulation of a trehalose-related sugar signal or through a direct role as a transcriptional regulator (Satoh-Nagasawa et al., 2006). Maize, together with sorghum and sugarcane, belongs to the Andropogoneae tribe, a group of grasses that develop spikelet pairs. In rice and other more distantly related grasses, spikelets are single, and no *RA1* homologue has been identified (Vollbrecht et al., 2005). This led to the hypothesis that the *ramosa* pathway and, in particular *RA1*, plays a central role in the evolution of grass inflorescence morphologies (Kellogg, 2007; McSteen, 2006; Vollbrecht et al., 2005). Despite genetic and expression analysis that place both *RA2* and *RA3* genes upstream of *RA1* in regulating spikelet-pair meristem identity and fate (Bortiri et al., 2006; Satoh-Nagasawa et al., 2006; Vollbrecht et al., 2005), it is unclear how this recently discovered pathway is operating.

MATERIALS AND METHODS

Mutagenesis, crosses and phenotyping

The *ra1-RS* allele was originally identified while screening a maize population in an undefined genetic background containing active transposable elements of the *Spm* family. In the course of this research, we determined (by searching for polymorphic markers) that this genetic background is closely related to the inbred line A619. Pollen was collected from *ra1-RS* homozygous plants and treated with 0.06% ethyl

[1]Section of Cell and Developmental Biology, University of California San Diego, La Jolla, CA 92093-0116, USA. [2]Plant Biology Laboratory, The Salk Institute for Biological Studies, La Jolla, CA 92037, USA. [3]Department of Genetics, Development and Cell Biology, Iowa State University, Ames, IA 50011-3260, USA. [4]Cold Spring Harbor Laboratory, Cold Spring Harbor, NY 11724, USA.

*Authors for correspondence (agallavotti@ucsd.edu; rschmidt@ucsd.edu)
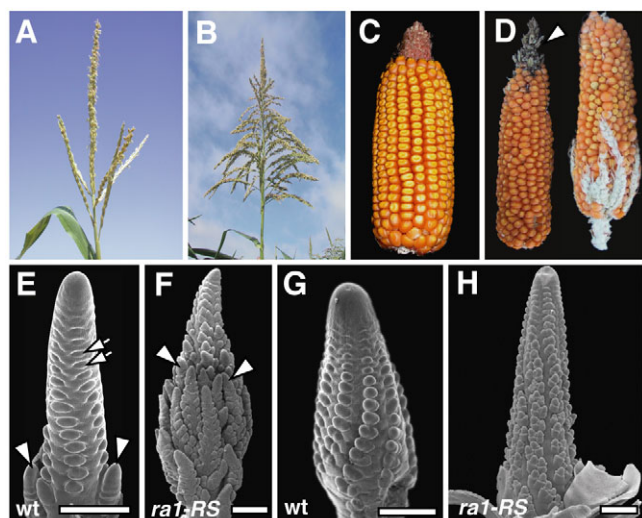
Fig. 1. Inflorescence development in normal and *ra1-RS* plants.
(**A**) Wild-type tassel. (**B**) *ra1-RS* tassel. (**C**) Wild-type ear. (**D**) *ra1-RS* ears; arrowhead indicates the masculinized tip. (**E-H**) Scanning electron microscopy (SEM) of wild-type and *ra1-RS* inflorescences. (E) Wild-type tassel with branch meristems (arrowheads) and spikelet-pair meristems (arrows). (F) *ra1-RS* tassel with extra developing branch meristems (arrowheads). Wild-type (G) and *ra1-RS (H)* ears. Scale bars: 500 μm.

methanesulfonate (EMS) in paraffin oil according to Neuffer (Neuffer, 1994). *ra1-RS* ears were then fertilized with the treated pollen using a brush. The resulting M1 plants were self-fertilized in order to create M2 families to be screened for enhanced and suppressed *ra1-RS* phenotypes (30 plants per family). For the double and triple mutant combinations, we used the following alleles: *rel2-ref*; *ra1-RS*; *ra1-63.3359*; *ra2-ref* introgressed in A619 (Vollbrecht et al., 2005; Bortiri et al., 2006). Tassel and ear branch numbers were determined by counting all primary branches, considered as any branch carrying more than two spikelets. Secondary branches are considered any branch, as defined above, arising from primary branches. The statistical significance of the differences in branch number was analyzed using Student's *t*-test.

Mapping, genotyping and expression analysis
For map-based cloning of *REL2*, a back-cross population was generated by crossing *rel2;ra1-RS* plants and the inbred line B73. Close linkage to Simple Sequence Repeat (SSR) marker umc1962 was used to develop additional markers as described elsewhere (Gallavotti et al., 2008) (see Fig. S3 and Table S4 in the supplementary material). For double and triple mutant combinations, we genotyped all plants with gene-specific markers (see Table S5 in the supplementary material).

For in situ hybridization, we used an antisense probe designed on the 3′ untranslated region of the *REL2* gene amplified using the following primers: REL2-3′UTR-F ATCTGATCAGCCAACAAGGTG and REL2-3′UTR-R ATCCATCAAATAGCCCCAAAC. RT-PCR and in situ hybridization expression analysis were performed as previously described (Gallavotti et al., 2008). *REL2* and *KNOTTED1* (*KN1*) RT-PCR primer sequences are provided in Table S6 in the supplementary material.

Scanning electron microscopy (SEM) and histology
For scanning electron microscopy immature inflorescences were fixed in FAA (50% ethanol, 3.7% formaldehyde, 5% acetic acid), dehydrated in a graded ethanol series, critically point dried and coated with a gold/palladium mixture. Images were taken with a Quanta 600 scanning electron microscope at 20 kV. We also used a Hitachi S-3500N environmental scanning electron microscope on freshly dissected inflorescences at 5 kV.

For histological sections of the pulvinus (Galinat, 1959), tassel branch nodes were collected prior to anthesis, immediately after the tassel fully emerged from the flag leaf, in order to avoid complete lignification of the

tissue. They were fixed in FAA, dehydrated in a graded ethanol series, treated with Histoclear and embedded in paraplast. Sections (8 μm) were placed on slides, dewaxed and stained with a Saffranin O/Alcian Blue solution (0.01%/0.05%), followed by rinsing in water. The sections were finally mounted in Permount (Fisher Scientific).

Protein-protein interaction assays
The following constructs were used for protein-protein interaction assays: *REL2ΔWD40* corresponds to +1 to +1022 nucleotide of the *REL2*-coding sequence; for *REL2ΔCTLH* and *REL2ΔCTLHΔWD40s*, nucleotides +109 to +276 were deleted from the coding sequence; for *RA1ΔEAR* and *RA1Δ2EAR*, the coding sequence was truncated at positions +496 and +298, respectively; for *RA1 mEAR*, the central EAR motif was changed to LDFEFRF (original sequence LDLELSL) and the C-terminal EAR motif was changed to LDFQFRF (original sequence LDLQLRL); for *RA1-RS* and *RA1-RSenh*, the coding sequence starts at position +28; for *RA1-63.3359*, the coding sequence includes an extra 17 amino acids at the C terminus (VLSQTEERTATMGTCSA).

For targeted yeast 2-hybrid assays, prey genes were cloned in the pAD-GAL4 2.1 vector, whereas bait genes were cloned in the pBD-GAL4 CAM vector (Stratagene). Interactions were assayed by growth on histidine-lacking media and by β-galactosidase activity, according to manufacturer's instructions (Stratagene). β-Galactosidase activity was quantified as previously described (Reynolds and Lundblad, 1987). Transient assays in tobacco were performed as previously described (Szemenyei et al., 2008). Constructs were prepared as N-terminal fusions in the SPYNE (N-terminal YFP fragment) and SPYCE (C-terminal YFP fragment) vectors of the Bimolecular Fluorescence Complementation (BiFC) system (Walter et al., 2004). Pull-down assays were performed using the MagneGST Pull-Down System (Promega) following manufacturer's instructions. For in vitro transcription/translation reactions, samples were incubated with bound GST (Glutathione S-transferase) fusions for ~2-4 hours, rotating at 4°C. For pull-down assays from leaf plant extracts, tobacco leaf were injected with Agrobacterium expressing the viral suppressor p19 (Voinnet et al., 2003) together with a *2X35S::RA1:MYC:NYFP* construct, and after 4 days the leaves were collected and ground for crude protein extraction. Incubations were performed overnight, rotating at 4°C. To express GST:REL2ΔWD40s fusion protein, the *REL2* gene was cloned as C-terminal fusions in pGEX-2TK (GE Healthcare). A 3×HA epitope tag (HA3) was added as a C-terminal fusion to RA1 in the pCITE vector (Novagen) and used for in vitro transcription/translation reactions.

For western blots we used mouse monoclonal anti-HA (Covance) and anti-GST (Cell Signaling Technology) antibodies at 1:2000 and 1:6000 dilutions, respectively, and a rabbit polyclonal anti-MYC (Cell Signaling Technology) antibody at 1:3000 dilution. For secondary antibodies we used 1:5000 to 1:10000 dilutions. For detection we used the ECL Plus Western Blotting Detection System (GE Healthcare).

In planta repression assay
The in planta repression assay and the TOPLESS promoter have been described by Szemenyei et al. (Szemenyei et al., 2008).

RESULTS
The discovery of the *ramosa1 enhancer locus2* mutant, a genetic enhancer of *ramosa1*
To uncover new genes in the *ramosa* pathway, we carried out an EMS-based mutagenesis on a weak allele of *ra1*, designated *ra1-RS* (Vollbrecht et al., 2005). *ra1-RS* tassels have an increase in branching compared with normal tassels as a result of the indeterminacy of spikelet-pair meristems (Fig. 1A,B,E,F) (Vollbrecht et al., 2005). Ear development is also affected, showing disorganized rows of seeds on the mature cob and the occasional formation of basal branches from the outgrowth of spikelet-pair meristems (Fig. 1C,D,G,H). Masculinization at the tip of the ear is also frequently observed (Fig. 1D). We screened ~1800 M2 families for an increase in tassel and ear branching, and we identified several mutations enhancing inflorescence branching.
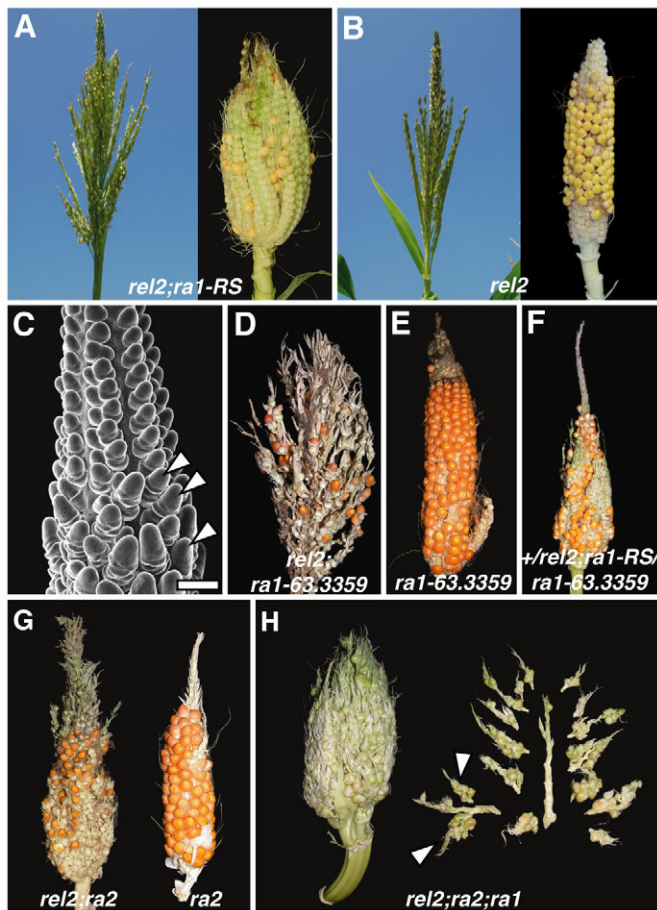
Fig. 2. The *rel2* mutant is a genetic enhancer of *ramosa1* and *ramosa2* mutants. (**A**,**B**) Double and single *rel2* mutant inflorescences (tassel, left; ear, right). (**C**) SEM of an immature *rel2;ra1-RS* ear, showing a proliferation of branch meristems (arrowheads) in place of spikelet-pair meristems. Scale bar: 200 μm. (**D**) *rel2;ra1-63.3359* ear phenotype. (**E**) *ra1-63.3359* mutant ear. (**F**) Heterozygous effect of *rel2* mutation in *ra1* mutants. Example of a dose effect of *rel2* in ear branching. (**G**) *rel2* enhances (left) the branched ear phenotype of a weak allele of *ra2* (right). (**H**) Triple *rel2;ra2;ra1* mutant ear. Primary branches form indeterminate secondary (right) and occasionally tertiary branches (arrowheads).

Among these, one recessive mutation affecting both tassel and ear branching was named *ramosa1 enhancer locus2* (*rel2*). *rel2;ra1-RS* double mutant plants showed highly branched ears and had tassels with distinctive upright branches (Fig. 2A). In developing ears, spikelet-pair meristems were indeterminate and converted into elongated branches (Fig. 2C). *rel2* and *rel2;ra1-RS* tassels also showed an increase in the number of primary branches (see Fig. S1 in the supplementary material). The *rel2* single mutant retained upright primary branches in the tassel but did not significantly affect ear branching (Fig. 2A,B). To determine whether the enhancement of ear branching was specific to the weak *ra1-RS* allele, which encodes a predicted RA1 protein that lacks the first nine amino acids (Vollbrecht et al., 2005), we created a double mutant with another characterized weak allele of *ra1*, designated *ra1-63.3359* (Vollbrecht et al., 2005). The C terminus of the predicted RA1-63.3359 protein has an extra 17 amino acids (Vollbrecht et al., 2005). *rel2;ra1-63.3359* mutant ears showed a

strong enhancement of branching (Fig. 2D). Analysis of this cross revealed that in +/*rel2;ra1-63.3359/ra1-63.3359* and +/*rel2;ra1-RS/ra1-63.3359* plants, ear branching was also enhanced when compared with either single *ra1-63.3359* mutants or +/*rel2;ra1-RS/ra1-RS* plants (Fig. 2E,F; see Fig. S1 in the supplementary material). Plants carrying the *ra1-63.3359* allele were therefore more sensitive to the lack of a functional copy of *REL2*. In a specific sensitized genetic background, therefore, the *rel2* mutation shows a semi-dominant effect.

### *rel2* enhances the branched phenotype of the *ramosa2* mutant
The *ra2* mutant was reported to enhance the *ra1-RS* mutant phenotype (Vollbrecht et al., 2005). We therefore crossed the *rel2-ref* mutant with an allele of *ra2* with a weaker phenotype. The resulting *rel2;ra2* double mutant plants showed an enhancement of ear branching relative to either single mutant (Fig. 2G; see Table S1 in the supplementary material). This enhancement was significant, although not as severe as in *rel2;ra1-RS* double mutants. We then generated *rel2;ra1;ra2* triple mutant plants. In these plants, the ears were characterized by a massive proliferation of branches. This was due to the indeterminacy of all spikelet-pair meristems, including those borne on branch meristems, resulting in the formation of primary, secondary and, occasionally, tertiary branches (Fig. 2H, see Table S2 in the supplementary material). Similar defects were also observed in *ra1;ra2* double mutants (Vollbrecht et al., 2005) (see Table S3 in the supplementary material) and in strong *ra1* alleles, such as *ra1-r* (see Fig. S2 in the supplementary material), suggesting that the *rel2;ra1-RS* ear phenotype can still be enhanced by the *ra2* mutation.

The *ra2* mutant also has a similar upright branch phenotype to *rel2* (Bortiri et al., 2006), independent from *ra1* (Fig. 3G). We therefore analyzed cross-sections of the tassel branch nodes in both *rel2* and *ra2* mutants. At the node where the tassel branch is connected with the central axis (spike), a group of cells forms a specialized structure called the pulvinus (Galinat, 1959), which swells at anthesis allowing branches to separate from the central spike and help the spreading of the pollen by the wind. Staining of these sections with Saffranin O and Alcian Blue, which stains lignified and non-lignified cell walls red and blue, respectively, revealed a group of red staining cells within the nodes of the *rel2* and *rel2;ra1-RS* mutants that was absent from either wild-type or *ra1-RS* plants (Fig. 3A-F). On their adaxial side, a variable number of small and unorganized vascular bundles is observed. In wild type or *ra1-RS* mutants, those additional vascular bundles were absent (Fig. 3E,F). However, blue staining of the pulvinal cells revealed that those cells seem unaffected. The presence of patches of lignified cells at the base of tassel branches in the *rel2* mutants is likely to cause a lack of flexibility in this area, forcing the tassel branches to develop upright. Given the similar upright branch phenotype of *ra2* mutants, we also sectioned and stained *ra2* tassels. More severe defects, such as misplaced pulvinal cells, were observed in *ra2* tassel branch nodes (Fig. 3G-I). The different structural and cellular organization in the two mutants suggests that *rel2* and *ra2* differentially affect the growth of tassel branches.

REL2 encodes a transcriptional co-repressor homologous to TOPLESS of *Arabidopsis*
We isolated the *REL2* gene by positional cloning and identified nonsense mutations in three independent alleles of *rel2* (*rel2-ref*, *rel2-SLO73*, *rel2-SLO335*) (Fig. 4A; see Fig. S3 in the
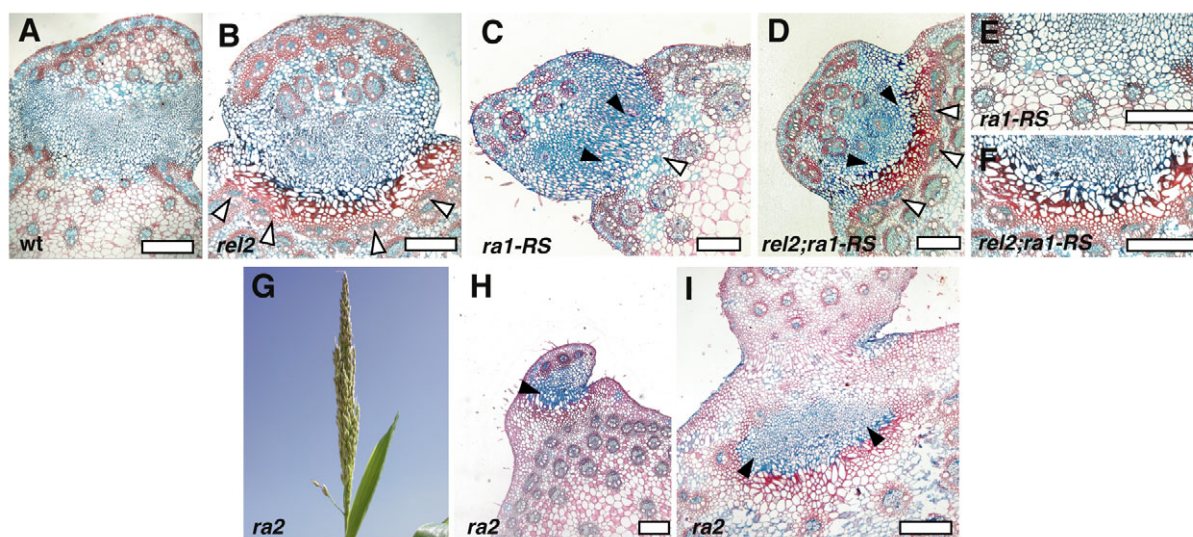
Fig. 3. The upright tassel branch phenotype of *rel2* and *ra2* mutants. (**A-F**) Cross-sections of the branch nodes in *rel2* and *rel2;ra1-RS* mutants, stained with Saffranin O and Alcian Blue. (**G**) *ra2* mutant tassel. (**H,I**) Cross-section of *ra2* tassel branch nodes. White arrowheads indicate vascular strands (B,D) or lack of vascular strands (C). Black arrowheads indicate pulvinal cells. Scale bars: 200 μm.

supplementary material). *REL2* is composed of 25 exons, and encodes a protein of 1141 amino acids with 66% identity to the transcriptional co-repressor TOPLESS (TPL) of *Arabidopsis* (Long et al., 2006) (Fig. 4A). *TPL* belongs to a family of five redundant members in *Arabidopsis*, and has been shown to function in the auxin signaling pathway for the maintenance of apical fate during embryogenesis (Szemenyei et al., 2008). Transcriptional co-repressors lack DNA-binding ability but are recruited by specific transcription factors to regulate gene expression of their target genes (Liu and Karmarkar, 2008). The domain organization of the REL2 protein resembles the one described for TPL (Long et al., 2006; Szemenyei et al., 2008) (Fig. 4A). The N terminus is characterized by two domains, the LisH (lyssencephaly type1-like homology) and the CTLH (C-terminal to LisH) domains. Following a proline-rich region of unknown function, eleven WD40 repeats are found in the C-terminal REL2 sequence. Notably, the CTLH domain of TPL is necessary for the interaction with the EAR repressor motif of the AUX/IAA proteins (Szemenyei et al., 2008), a class of transcriptional repressors of early auxin responsive genes (Overvoorde et al., 2005). AUX/IAA proteins form heterodimers with the ARF transcription factors (Hardtke et al., 2004; Overvoorde et al., 2005), and, by recruiting TPL, they repress transcription of ARF target genes (Smith and Long, 2010; Szemenyei et al., 2008). RT-PCR (see Fig. S3 in the supplementary material) and in situ hybridizations of *REL2* in developing maize inflorescences showed a ubiquitous signal, with stronger expression in meristematic tissues, such as inflorescence, branch and spikelet-pair meristems (Fig. 4B,C,E,F), in developing floral organs and in the vasculature (Fig. 4D).

To verify that *REL2* functions as a transcriptional co-repressor, we tested whether or not *REL2* was capable of rescuing the embryonic defects of the temperature-sensitive *tpl-1* mutant (Long et al., 2006; Szemenyei et al., 2008). *tpl-1* embryos show a range of phenotypes, such as single fused cotyledons (Fig. 4G) and, in the most severe cases, a root in place of a shoot – hence the name (Long et al., 2002). We transformed *tpl-1* plants with a construct expressing a REL2-YFP fusion protein under the control of the

endogenous TPL promoter (*pTPL::REL2:YFP*). Seven independent lines showed a complete rescue of the *tpl-1* embryonic defects, and nuclear localization of the REL2-YFP fusion protein, consistent with a role in transcriptional regulation (Fig. 4G-J). We subsequently tested whether REL2 was capable of repressing the transcription of a β-glucoronidase (GUS) reporter gene in an in planta repression assay (Szemenyei et al., 2008) and we observed decreased GUS activity (Fig. 4K,L). Taken together, these results demonstrate that REL2 is a transcriptional co-repressor.

REL2 and RA1 physically interact

In our screen for the enhancement of inflorescence branching, we also identified an intragenic enhancer of the *ra1-RS* mutation (Fig. 5). We discovered a C475T transition in the *ra1-RS* coding sequence that caused the replacement of one leucine with a phenylalanine in the conserved C-terminal EAR-like repressor motif (LxLxLx) of the RA1 protein (Vollbrecht et al., 2005) (Fig. 5A). EAR repressor motifs have been described in several families of transcriptional regulators, such as the zinc-finger SUPERMAN (SUP) and the AUX/IAA proteins (Hiratsu et al., 2004; Tiwari et al., 2004). This mutant, renamed *ra1-RSenh*, showed a dramatic increase in ear branching owing to the conversion of spikelet-pair meristems into branch meristems (Fig. 5B,C), indicating that the leucine in the C-terminal EAR motif is crucial for function and suggesting that a transcriptional repressor mechanism regulates the establishment of spikelet-pair meristem determinacy. The RA1 protein also carries another potential EAR motif (LDLELSL, amino-acids 100-106), distal to the Zn-finger domain.

The discovery that *REL2* encodes a transcriptional co-repressor with a CTLH domain, and that the RA1 protein carries two putative EAR motifs, at least one of which is important for RA1 function, prompted us to investigate whether the REL2 and RA1 proteins physically interact. We first tested this hypothesis using a targeted yeast 2-hybrid assay, and we detected interaction between RA1 and full-length REL2, as well as a truncated version of REL2 (REL2ΔWD40). The presence of the CTLH domain of REL2 was required, as evidenced by the loss of interaction when expressing REL2 proteins that lacked this domain (REL2ΔCTLH,
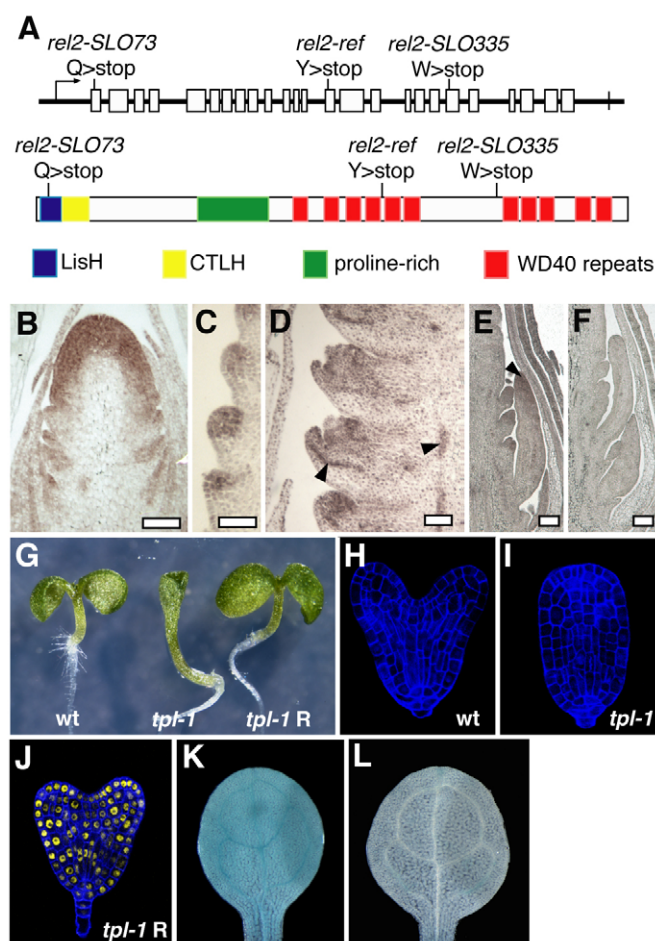
Fig. 4. *REL2* encodes a transcriptional co-repressor. (**A**) Schematic representation of the *REL2* gene (above) and of the encoded protein (below). The three isolated independent *rel2* mutant alleles and the corresponding mutations are indicated. White boxes represent exons. Colored boxes represent different domains of the REL2 protein: lyssencephaly type1-like homology (LisH); C-terminal to LisH (CTLH). (**B-F**) In situ hybridization of *REL2* during inflorescence development. (B) Young developing ear. (C) Spikelet-pair meristems. (D) Floral meristems developing floral organs; *REL2* expression is also visible in the vasculature (arrowheads). (E,F) Branch meristem (arrowhead) of a young developing tassel; antisense (E) and sense control (F). Scale bars: 50 µm. (**G**) *REL2* rescues the *tpl-1* phenotype of *Arabidopsis*. One representative line is shown (*tpl-1* R). (**H-J**) Confocal images of wild-type, *tpl-1* and *tpl-1* embryos rescued by REL2-YFP (*tpl-1* R). (**K,L**) In planta repression assay. We transformed an *Arabidopsis* line carrying the reporter construct *2xUAStCUP::GUS* (Szemenyei et al., 2008) (K) with another construct expressing REL2 fused to the DNA-binding domain (DB) of the yeast GAL4 transcriptional activator (*pTPL::REL2:GAL4DB:HA*). Staining in cotyledons shows that REL2:GAL4DB (L) is capable of repressing the expression of GUS.

RELΔWD40ΔCTLH) (Fig. 6A,B). Mutations specifically affecting the C terminus of the RA1 protein (RA1-RSenh, RA1-63.3359, RA1ΔEAR) resulted in a weaker interaction with REL2 when compared with RA1 or RA1-RS proteins (Fig. 6A,B; see Fig. S4 in the supplementary material). The interaction was completely abolished only if RA1 was missing the C terminus (RA1Δ2EAR) or when mutations were introduced in both EAR motifs simultaneously (RA1mEAR) (Fig. 6B). To test the interaction in
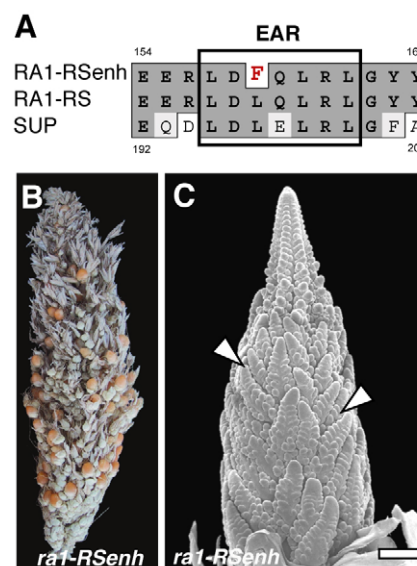
Fig. 5. The *ra1RSenh* allele is an intragenic enhancer of *ra1-RS*. (**A**) ClustalW alignment of the EAR repressor motifs of *ra1-RSenh*, *ra1-RS* and the SUPERMAN (SUP) proteins of *Arabidopsis*. (**B**) *ra1-RSenh* highly branched ear. (**C**) Scanning electron microscopy image of an immature *ra1-RSenh* ear showing a proliferation of branch meristems (arrowheads). Scale bar: 500 µm.

planta, we used a bimolecular fluorescence complementation (BiFC) system for transient expression in tobacco leaves (Walter et al., 2004), and verified that REL2 and RA1 interact in the nucleus and confirmed that the interaction depends on the two EAR motifs (REL2-CYFP/RA1mEAR-NYFP) (Fig. 6C). We also tested the REL2/RA1 interaction by pull-down assays, using beads bound to a GST:REL2ΔWD40 bacterial expressed protein or to GST alone. Both in vitro expressed RA1:HA3 (Fig. 6D) and in planta expressed RA1:MYC:NYFP fusion proteins (Fig. 6E) were recovered using GST:REL2ΔWD40 bound beads, but not with GST alone. These results show that REL2 and RA1 can physically interact in both in vitro and in vivo assays. We also tested REL2 together with RA2 or RA3 proteins in yeast 2-hybrid and BiFC assays, but no interaction was detected (data not shown).

DISCUSSION

Plant development relies on the activity of meristems, highly organized and regulated groups of stem cells responsible for the formation of all post-embryonic organs. Whereas the shoot and the root apical meristems, formed during embryogenesis, establish the main axis of plant growth (apical to basal), axillary meristems are responsible for the formation of secondary axes of growth, such as branches and flowers. The outcome of axillary meristem activity is a crucial component of what determines the architectural variation observed in different plant species.

In this paper, we described one molecular mechanism by which an axillary meristem can acquire a determinate fate and result in the formation of a pair of spikelets, the defining units of grass inflorescences and the source of maize productivity. Based on our genetic and molecular data, we propose a model for maize spikelet-pair meristem determinacy in which RA1 recruits REL2 to the promoter of its target genes via an interaction involving two EAR repressor motifs and the CTLH domain of the REL2 protein (Fig.
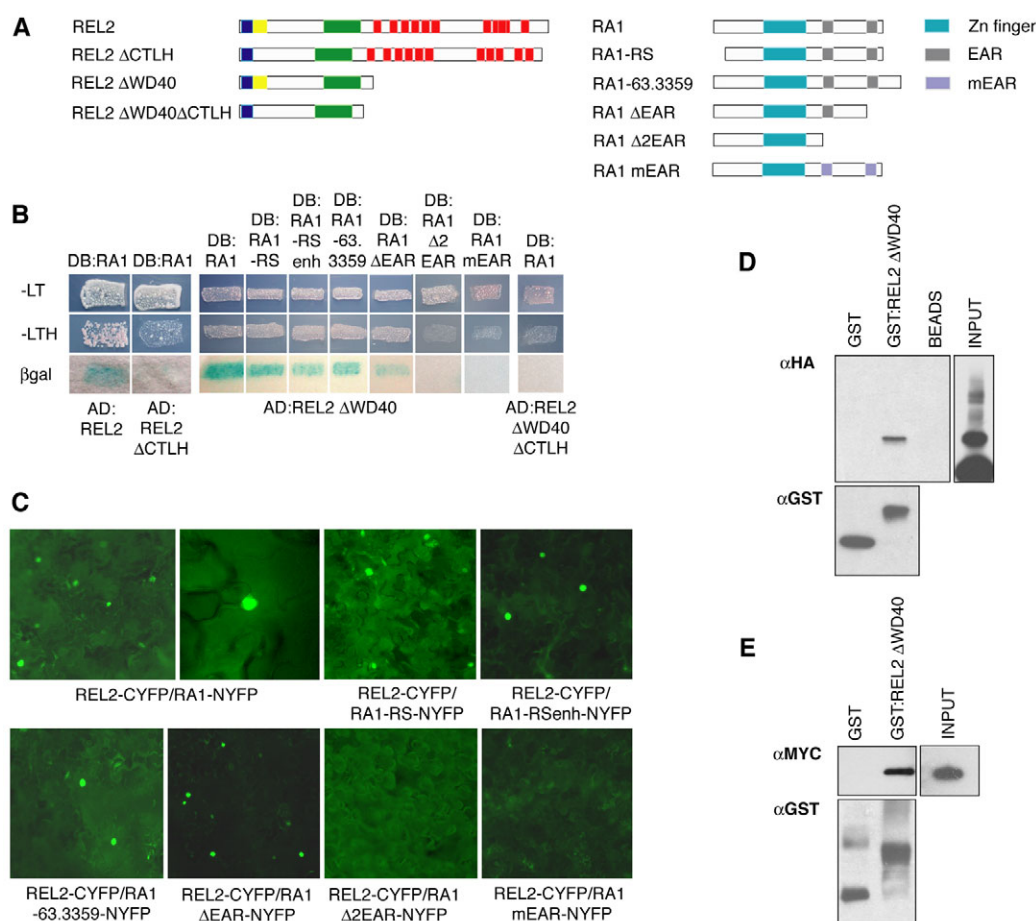
Fig. 6. REL2 and RA1 interact in vivo and in vitro. (**A**) Schematic representations of the modified versions of REL2 and RA1 proteins used in protein-protein interaction assays. (**B**) Targeted yeast 2-hybrid assay. Yeast transformants are grown in the selection medium (–LT). The interaction is tested on histidine-lacking medium (–LTH) and by β-galactosidase (βgal) activity. AD, GAL4 activation domain; DB, GAL4 DNA-binding domain. (**C**) In planta bi-fluorescent complementation assay. Transient expression in tobacco leaves. (**D**) Pull-down assay of in vitro transcribed/translated *RA1:HA3* (input). (**E**) Pull-down assay of in vivo transcribed/translated *RA1:MYC:NYFP* (input). In D,E, input lanes represent one-tenth of the volume used for the assay.

7). The physical interaction between the C-terminal end of the RA1 protein and REL2 is supported by genetic evidence such as the haploinsufficiency of *REL2* observed in the *ra1-63.3359* mutant, and by the highly branched phenotype of the *ra1-RSenh* mutant. Although the targets of RA1 binding remain unknown, several mutations in the zinc-finger DNA-binding domain have been identified and show a strong *ra1* phenotype (Cassani et al., 2006; Vollbrecht et al., 2005) (see Fig. S2 in the supplementary material). The reported absence of RA1 expression in the tassel branch meristems (Vollbrecht et al., 2005) is in agreement with this model, whereby no repression mechanism is in place and indeterminacy is maintained. It is likely that, as in *Arabidopsis* (Long et al., 2006), other REL2-like proteins act in a partially redundant manner in this pathway, which could explain why *rel2* single mutants do not show enhanced ear branching. In *rel2;ra1-RS* mutants, the expression of *REL2* is unchanged (see Fig. S3 in the supplementary material). This suggests that a truncated REL2-REF protein could still be present and interact with the RA1-RS protein, but the complex would have impaired repressing function. The enhancement of the *rel2;ra1-RS* ear mutant phenotype by the *ra2* mutation indeed suggests that the REL2-REF/RA1-RS complex is still partially functional. Similarly, in the *ra1-RSenh* mutant, the interaction

between REL2 and the mutant RA1-RSenh protein is likely not completely lost (Fig. 6), and no enhancement of secondary branches is indeed observed (data not shown).

Transcriptional repression is rapidly emerging as a common theme in the control of developmental processes in plants (Liu and Karmarkar, 2008; Krogan and Long, 2009). In this paper, we show that the regulation of axillary meristem fate can occur by a transcriptional repression mechanism involving the interaction of an EAR-containing zinc-finger transcription factor and the REL2 transcriptional co-repressor. Two fundamental and distinct pathways, the control of meristem fate (described here) and the establishment of embryo polarity (Smith and Long, 2010; Szemenyei et al., 2008), employ the same type of transcriptional co-repressor, the recruitment of which is guided by different and unrelated transcription factors via EAR-repressor motifs. A similar mechanism has also been recently described in *Arabidopsis* for the signaling pathway of the plant hormone jasmonate (Pauwels et al., 2010). What seems to differ are the number and nature of the proteins involved in the assembly of the repressor complex, as well as the mode of interaction. Whereas in the case of the auxin signaling pathway three proteins are involved (TPL, AUX/IAAs and ARFs) (Szemenyei et al., 2008), in the jasmonate signaling
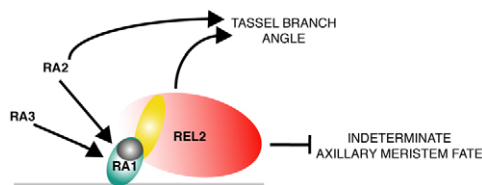
Fig. 7. Proposed model for the repression of the indeterminate fate of spikelet-pair meristems. REL2 and RA1 form a complex, interacting via the two EAR motifs (grey) and the CTLH domain (yellow). This complex represses the expression of target genes (grey solid bar), resulting in the determinacy of spikelet-pair meristems. *RA2* and *RA3* have been previously shown to regulate *RA1* transcript levels (Bortiri et al., 2006; Satoh-Nagasawa et al., 2006). *REL2* and *RA2* also differently affect, independently from *RA1*, the angle of tassel branches.

pathway four proteins have been reported as being part of the repressor complex (Pauwels et al., 2010). However, in the *ramosa* pathway, RA1 and REL2 may be the only proteins required, and, only in this case, two EAR motifs are implicated in the interaction.

The fine regulation of the balance between differentiation and stem cell proliferation determines whether a meristem acquires a determinate or an indeterminate fate (Sablowski, 2007a; Sablowski, 2007b). In *Arabidopsis*, the homeodomain protein WUSCHEL (WUS) is well known to maintain the pools of meristematic stem cells (Mayer et al., 1998; Sablowski, 2007b). During reproductive development, in the determinate floral meristems the function of *WUS* eventually has to be terminated to form all floral organs. The floral homeotic gene *AGAMOUS* (*AG*) is indeed necessary for the termination of *WUS* activity (Lenhard et al., 2001; Lohmann et al., 2001). Recently, it has been proposed that AG activates the transcription of the zinc-finger transcription factor *KNUCKLES* (*KNU*), which contains a C-terminal EAR motif that in turn negatively regulates *WUS*. The timing of *KNU* expression has been associated with the regulation of meristem fate, as delayed *KNU* expression results in the formation of indeterminate meristems, whereas ectopic expression results in premature termination of floral meristems (Sun et al., 2009). This effect has also been reported for *RA1*, where changes in the timing of expression have been correlated to changes in the inflorescence architecture of some maize alleles and of related grasses, such as sorghum (Vollbrecht et al., 2005). These similarities may suggest that *KNU* functions similarly to *RA1*, and therefore, expanding the analogy, that the REL2/RA1 complex may repress *WUS*-like activity in meristems, promoting differentiation at the expense of meristem maintenance. Although the maize orthologs of *WUS* are not expressed in the same domain as *RA1* (Nardmann and Werr, 2006), *RA1* was shown to function non cell-autonomously by sector analysis (Vollbrecht et al., 2005). It is important to note, though, that the architecture of maize and *Arabidopsis* inflorescences is very distinct. Unlike in *Arabidopsis*, where floral meristems form directly at the flanks of the inflorescence meristem, maize spikelet-pair meristems give rise to a series of axillary meristems (spikelet and floral meristems) that eventually form flowers (McSteen et al., 2000). Whereas in weak *ra1* mutants, spikelet meristems are also slightly indeterminate, causing the formation of ears with unorganized rows (Vollbrecht et al., 2005; Cassani et al., 2006), determinate floral meristems eventually form. A series of genes, mostly transcription factors, that specifically regulate the identity and fate of these additional meristems have been characterized (Chuck et al., 1998; Chuck et al., 2002; Chuck et al., 2007; Chuck et al., 2008;

Thompson et al., 2009), highlighting the existence of multiple regulatory pathways controlling the determinacy of most reproductive axillary meristems.

The activity and development of axillary meristems determine the diversity observed in the body plans and in the inflorescences of different plant species, therefore affecting productivity and the needs of modern agriculture. The identification of REL2 and of its physical interaction with RA1 sheds light on the molecular mechanisms that underlie different inflorescence architectures in grasses, and provides useful knowledge for modern breeding and for the improvement of crop species.

Competing interests statement

The authors declare no competing financial interests.

Supplementary material

Supplementary material for this article is available at
http://dev.biologists.org/lookup/suppl/doi:10.1242/dev.051748/-/DC1

References

Bortiri, E., Chuck, G., Vollbrecht, E., Rocheford, T., Martienssen, R. and Hake, S. (2006). ramosa2 encodes a LATERAL ORGAN BOUNDARY domain protein that determines the fate of stem cells in branch meristems of maize. *Plant Cell* **18**, 574-585.

Cassani, E., Landoni, M. and Pilu, R. (2006). Characterization of the Ra1 maize gene involved in inflorescence architecture. *Sex. Plant Reprod.* **19**, 145-150.

Chuck, G., Meeley, R. B. and Hake, S. (1998). The control of maize spikelet meristem fate by the APETALA2-like gene indeterminate spikelet1. *Genes Dev.* **12**, 1145-1154.

Chuck, G., Muszynski, M., Kellogg, E., Hake, S. and Schmidt, R. J. (2002). The control of spikelet meristem identity by the branched silkless1 gene in maize. *Science* **298**, 1238-1241.

Chuck, G., Meeley, R., Irish, E., Sakai, H. and Hake, S. (2007). The maize tasselseed4 microRNA controls sex determination and meristem cell fate by targeting Tasselseed6/indeterminate spikelet1. *Nat. Genet.* **39**, 1517-1521.

Chuck, G., Meeley, R. and Hake, S. (2008). Floral meristem initiation and meristem cell fate are regulated by the maize AP2 genes ids1 and sid1. *Development* **135**, 3013-3019.

Galinat, W. (1959). The phytomer in relation to the floral homologies in the American Maydea. *Bot. Mus. Leafl. Harv. Univ.* **19**, 1-32.

Gallavotti, A., Barazesh, S., Malcomber, S., Hall, D., Jackson, D., Schmidt, R. J. and McSteen, P. (2008). sparse inflorescence1 encodes a monocot-specific YUCCA-like gene required for vegetative and reproductive development in maize. *Proc. Natl. Acad. Sci. USA* **105**, 15196-15201.

Hardtke, C. S., Ckurshumova, W., Vidaurre, D. P., Singh, S. A., Stamatiou, G., Tiwari, S. B., Hagen, G., Guilfoyle, T. J. and Berleth, T. (2004). Overlapping and non-redundant functions of the Arabidopsis auxin response factors MONOPTEROS and NONPHOTOTROPIC HYPOCOTYL 4. *Development* **131**, 1089-1100.

Hiratsu, K., Mitsuda, N., Matsui, K. and Ohme-Takagi, M. (2004). Identification of the minimal repression domain of SUPERMAN shows that the DLELRL hexapeptide is both necessary and sufficient for repression of transcription in Arabidopsis. *Biochem. Biophys. Res. Commun.* **321**, 172-178.

Kellogg, E. A. (2007). Floral displays: genetic control of grass inflorescences. *Curr. Opin. Plant Biol.* **10**, 26-31.

Krogan, N. T. and Long, J. A. (2009). Why so repressed? Turning off transcription during plant growth and development. *Curr. Opin. Plant Biol.* **12**, 628-636.

Lenhard, M., Bohnert, A., Jurgens, G. and Laux, T. (2001). Termination of stem cell maintenance in Arabidopsis floral meristems by interactions between WUSCHEL and AGAMOUS. *Cell* **105**, 805-814.

Liu, Z. and Karmarkar, V. (2008). Groucho/Tup1 family co-repressors in plant development. *Trends Plant Sci.* **13**, 137-144.

Lohmann, J. U., Hong, R. L., Hobe, M., Busch, M. A., Parcy, F., Simon, R. and Weigel, D. (2001). A molecular link between stem cell regulation and floral patterning in Arabidopsis. *Cell* **105**, 793-803.

Long, J., Woody, S., Poethig, S., Meyerowitz, E. and Barton, M. (2002). Transformation of shoots into roots in Arabidopsis embryos mutant at the TOPLESS locus. *Development* **129**, 2797-2806.

Long, J. A., Ohno, C., Smith, Z. R. and Meyerowitz, E. M. (2006). TOPLESS regulates apical embryonic fate in Arabidopsis. *Science* **312**, 1520-1523.

Mayer, K. F., Schoof, H., Haecker, A., Lenhard, M., Jurgens, G. and Laux, T. (1998). Role of WUSCHEL in regulating stem cell fate in the Arabidopsis shoot meristem. *Cell* **95**, 805-815.

McSteen, P. (2006). Branching out: the ramosa pathway and the evolution of grass inflorescence morphology. *Plant Cell* **18**, 518-522.

McSteen, P. and Leyser, O. (2005). Shoot branching. *Annu. Rev. Plant Biol.* **56**, 353-374.

McSteen, P., Laudencia-Chingcuanco, D. and Colasanti, J. (2000). A floret by any other name: control of meristem identity in maize. *Trends Plant Sci.* **5**, 61-66.

Nardmann, J. and Werr, W. (2006). The shoot stem cell niche in angiosperms: expression patterns of WUS orthologues in rice and maize imply major modifications in the course of mono- and dicot evolution. *Mol. Biol. Evol.* **23**, 2492-2504.

Neuffer, M. G. (1994). Mutagenesis. In *The Maize Handbook* (ed. M. Freeling and V. Walbot), pp. 212-219. New York: Springer-Verlang.

Overvoorde, P. J., Okushima, Y., Alonso, J. M., Chan, A., Chang, C., Ecker, J. R., Hughes, B., Liu, A., Onodera, C., Quach, H. et al. (2005). Functional genomic analysis of the AUXIN/INDOLE-3-ACETIC ACID gene family members in Arabidopsis thaliana. *Plant Cell* **17**, 3282-3300.

Pauwels, L., Barbero, G. F., Geerinck, J., Tilleman, S., Grunewald, W., Perez, A. C., Chico, J. M., Bossche, R. V., Sewell, J., Gil, E. et al. (2010). NINJA connects the co-repressor TOPLESS to jasmonate signalling. *Nature* **464**, 788-791.

Reynolds, A. and Lundblad, V. (1987). Assay for β-galactosidase in liquid cultures. In *Current Protocols in Molecular Biology*, Vol. 2 (ed. F. M. Ausubel, R. Brent, R. E. Kingston, D. D. Moore, J. G. Seidman, J. A. Smith and K. Struhl), pp. 13.6.2-13.6.4. New York: John Wiley and Sons.

Sablowski, R. (2007a). The dynamic plant stem cell niches. *Curr. Opin. Plant Biol.* **10**, 639-644.

Sablowski, R. (2007b). Flowering and determinacy in Arabidopsis. *J. Exp. Bot.* **58**, 899-907.

Satoh-Nagasawa, N., Nagasawa, N., Malcomber, S., Sakai, H. and Jackson, D. (2006). A trehalose metabolic enzyme controls inflorescence architecture in maize. *Nature* **441**, 227-230.

Smith, Z. R. and Long, J. A. (2010). Control of Arabidopsis apical-basal embryo polarity by antagonistic transcription factors. *Nature* **464**, 423-426.

Sun, B., Xu, Y., Ng, K. H. and Ito, T. (2009). A timing mechanism for stem cell maintenance and differentiation in the Arabidopsis floral meristem. *Genes Dev.* **23**, 1791-1804.

Szemenyei, H., Hannon, M. and Long, J. A. (2008). TOPLESS mediates auxin-dependent transcriptional repression during Arabidopsis embryogenesis. *Science* **319**, 1384-1386.

Thompson, B. E., Bartling, L., Whipple, C., Hall, D. H., Sakai, H., Schmidt, R. and Hake, S. (2009). bearded-ear encodes a MADS box transcription factor critical for maize floral development. *Plant Cell* **21**, 2578-2590.

Tiwari, S. B., Hagen, G. and Guilfoyle, T. J. (2004). Aux/IAA proteins contain a potent transcriptional repression domain. *Plant Cell* **16**, 533-543.

Voinnet, O., Rivas, S., Mestre, P. and Baulcombe, D. (2003). An enhanced transient expression system in plants based on suppression of gene silencing by the p19 protein of tomato bushy stunt virus. *Plant J.* **33**, 949-956.

Vollbrecht, E., Springer, P. S., Goh, L., Buckler, E. S., 4th and Martienssen, R. (2005). Architecture of floral branch systems in maize and related grasses. *Nature* **436**, 1119-1126.

Walter, M., Chaban, C., Schutze, K., Batistic, O., Weckermann, K., Nake, C., Blazevic, D., Grefen, C., Schumacher, K., Oecking, C. et al. (2004). Visualization of protein interactions in living plant cells using bimolecular fluorescence complementation. *Plant J.* **40**, 428-438.